Rayleigh Scattering Cluster Based Spatial-Temporal-Spectral Correlation Properties with MIMO-OFDM Channel Model

Xin Li and Torbjörn Ekman
Department of Electronics and Telecommunications
Norwegian University of Science and Technology
N-7491, Trondheim, Norway
{xin.li, torbjorn.ekman}@iet.ntnu.no

***Abstract*— This paper addresses the MIMO-OFDM channel simulator in state space representation which is based on the spatial-temporal-spectral correlation due to clustered radio propagation. The scattering clusters are assumed to be 2D Rayleigh clusters. This renders AOD, AOA that can be approximated as the Gaussian angular power distributions, and TOA that can be approached as the Gaussian delay power distribution. Thus, the spatial-temporal-spectral correlation can be approximated as the product of an AR(3) process and the corresponding spatial-spectral correlation. A state space model is used to the temporal dynamics of the MIMO channels. The contribution of the cluster to each antenna is a state in this model. A correlated innovation process adjusts the correlation between antennas and frequencies. This renders the appropriate spatial-temporal-spectral channel correlation in the simulated channels.**

Keywords: MIMO, OFDM, AOD, AOA, TOA, AR(3), Gaussian Distribution, State Space Model.

I. Introduction

Geometrically based statistical multiple-input and multiple-output (MIMO) channel modeling, providing a way of study the angle of arrival (AOA), angle of departure (AOD) and time of arrival (TOA), has received much attention [1]–[4]. The main idea is based on the assumption that the scatterers in a two-dimensional (2D) cluster are obeying some statistical characteristics, with which the geometrical relationships lead to the approached models by mapping the location statistics of the scatterers to the AOA, AOD and TOA.

The orthogonal frequency division multiplexing (ODFM) has become a popular technique for transmission of signals over wireless channels. The objective is converting a frequency-selective channel into a parallel collection of frequency flat sub-channels. The combination of MIMO and OFDM techniques has been considered for the physical layer transmission scheme of broad-band wireless communication systems [5].

An autoregressive order two, AR(2), process is commonly used to model the Doppler spectrum density function. Fitting it to the U-shape of the Jakes spectrum, it is used for fading channel identification and estimation [6], [7]. It is even used in MIMO- OFDM channel estimation [8]. In this paper, we model the contribution from a distant cluster of scatterers to the Doppler spectrum by an AR(3) process. The full Doppler spectrum can be generated by summing the contributions from AR(3) processes obtained form a number of uncorrelated scattering clusters.

A state space based single frequency MIMO channel simulator due to a 2D distant Rayleigh (DRH) scattering cluster is developed in [9]. In this paper, the factor of time delay is included in the DRH clustered radio propagation environment. This renders the TOA that can be approximately modeled as a Gaussian delay power density function for a small angular spread. The spatial-temporal-spectral correlation function is then decomposed by assuming the independent AOD, AOA and TOA. Thus, the MIMO-OFDM channel is approximately modeled by the state space MIMO channel model blocks as presented in [9], in which an innovation process is used to adjust the spatial corrections within each block and spectral correlations between the blocks.

In this paper, we restrict our studies to a 2×2 antenna configuration. Similar properties can be easily obtained for larger antenna arrays.

This paper is organized as follows. In Section II, the spatial-temporal-spectral correlation function is provided. In Section III, a 2D DRH scattering cluster is given, by which the AOD, AOA and TOA are modeled. In Section IV, the AR(3) process is presented. In Section V, the state space realization for an AR(3) process is presented. Simulation results are displayed in Section VI. Some of the derivations are provided in the Appendixes. Finally, Section VII concludes the paper.

II. Spatial-Temporal-Spectral Correlation Function

In order to study the channel spatial-temporal-spectral correlation properties, a 2×2 MIMO system is considered. This system is illustrated in Fig.1 on which the four antenna sensor to antenna sensor wireless connections are referred to as narrow-band channels and Fig.2 on which a distant scattering cluster and the geometrical relationship associated with the AOA and AOD are plotted. Assume that the base station (BS) is fixed while the mobile station (MS) is moving with the velocity v, and there is no line of sight (LOS) between the BS and MS, the links between them are set up by a scattering cluster, in which C is the cluster center, O is an arbitrary scatterer in the cluster. Then the channel vector at time t and frequency f $[h_{11}(t,f)\ h_{12}(t,f)\ h_{21}(t,f)\ h_{22}(t,f)]$ represents

978-1-4673-1881-5/12/$31.00 ©2012 IEEE

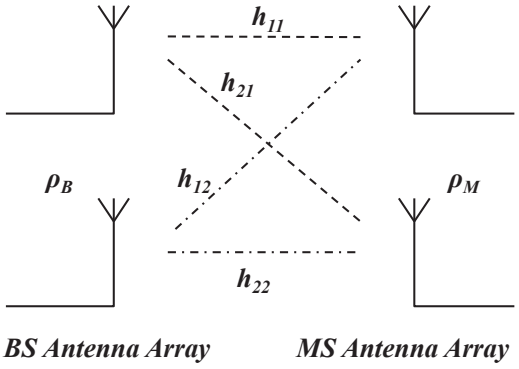

Fig. 1. A 2×2 MIMO System.

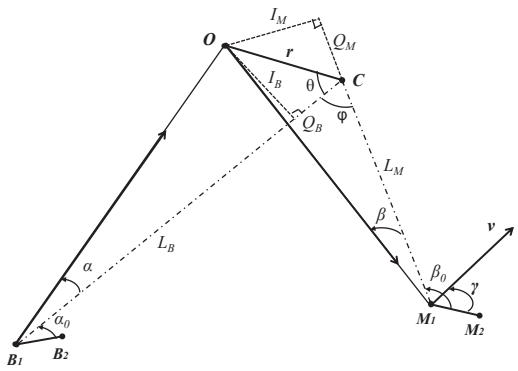

Fig. 2. A Distant Scattering Cluster with the Center C, an Arbitrary Scatterer O and a 2×2 Antenna Array.

the simplest MIMO structure, for which the spatial-temporal-spectral correlation function of the 2×2 MIMO channel is [10], [11]

$$C(\kappa, n, d_B, d_M) = \int_{\alpha,\beta,\tau} f_{\alpha,\beta,\tau}(\alpha,\beta,\tau) e^{j2\pi d_B \cos(\alpha+\alpha_0)} \cdot e^{j2\pi d_M \cos(\beta+\beta_0)} e^{-j2\pi\kappa\cos(\beta+\beta_0-\gamma)} e^{-j2\pi n\Delta f\tau} d\alpha d\beta d\tau \quad (1)$$

where $\alpha, \beta \in [-\pi\ \pi]$ are azimuth AOD, AOA with means α_0, β_0, respectively, τ denotes the time delay, $f_{\alpha,\beta,\tau}(\alpha,\beta,\tau)$ is the joint angular-delay power density function, γ is the angle between the moving direction and the MS antenna array (as illustrated in Fig.2), $\kappa = v\Delta t/\lambda$ denotes the traveled electrical distance, and d_B, d_M denote the spacing between the BS antenna sensors and MS antenna sensors, respectively, they are measured in wavelength [4], [12], [13], Δf denotes the difference of two adjacent sub-carrier frequencies. It is clear that the traveled electrical distance κ is frequency dependent, but it can be approximately treated as the same for all sub-carrier frequencies when the relative bandwidth is small.

Although α, β, τ are dependent, we assume the independence of α, β, τ, i.e., $f_{\alpha,\beta,\tau}(\alpha,\beta,\tau) = f_\alpha(\alpha) f_\beta(\beta) f_\tau(\tau)$ for the reason of obtaining the analytical approaches. Therefore, Eqn.(1) can be approximately expressed as [10]

$$\begin{aligned} C(\kappa, n, d_B, d_M) &\approx C_{ch}(\kappa, n, d_B, d_M) = e^{j2\pi d_B \cos(\alpha_0)} \\ &\cdot e^{j2\pi d_M \cos(\beta_0)} \int_\alpha f_\alpha(\alpha) e^{-j2\pi d_B \sin(\alpha_0)\alpha} d\alpha \\ &\cdot e^{-j2\pi\kappa\cos(\gamma-\beta_0)} \int_\tau f_\tau(\tau) e^{-j2\pi n\Delta f\tau} d\tau \\ &\cdot \int_\beta f_\beta(\beta) e^{-j2\pi d_M \sin(\beta_0)\beta} e^{-j2\pi\kappa\sin(\gamma-\beta_0)\beta} d\beta \end{aligned} \quad (2)$$

In the following section, we will specify the spatial-temporal-spectral correlation function (Eqn.(2)) for the case α, β, τ are Gaussian distributed.

III. Rayleigh Scattering Cluster with AOD, AOA, TOA Derivations

In this section, a 2D distant scattering cluster, named Rayleigh cluster, is introduced to model the AOD, AOA and TOA. It has been shown that for small angles α, β, the AOD and AOA are approximately modeled as the Gaussian angular power density functions if the 2D distant scattering cluster is Rayleigh distributed [9]. This models the case when the angular distribution has a smooth peak, which can be observed in some situations [14], [15].

The probability density function (PDF) of the DRH scattering cluster is given by

$$g_{r,\theta}(r,\theta) = \frac{1}{2\pi}\frac{r}{\sigma_r^2} e^{-\frac{r^2}{2\sigma_r^2}}, \quad r > 0,\ 0 \le \theta \le 2\pi, \quad (3)$$

where θ is uniformly distributed over 2π, r is referred to as the Rayleigh model. Triangular relationship gives that α, β can be approximately modeled by the Gaussian angular power density functions

$$g_\alpha(\alpha) \approx \frac{1}{\sqrt{2\pi}\sigma_b} e^{-\frac{\alpha^2}{2\sigma_b^2}}, \quad g_\beta(\beta) \approx \frac{1}{\sqrt{2\pi}\sigma_m} e^{-\frac{\beta^2}{2\sigma_m^2}} \quad (4)$$

where the variance $\sigma_b^2 = \sigma_r^2/L_B^2$ and $\sigma_m^2 = \sigma_r^2/L_M^2$. The derivation of Eqn.(4) can be found in [16]. The TOA can be approached by the Gaussian delay power density function

$$g_\tau(\tau) \approx \frac{1}{\sqrt{2\pi}\sigma} e^{-\frac{(\tau-\overline{\tau})^2}{2\sigma^2}} \quad (5)$$

where $\overline{\tau} = (L_M + L_B)/c$ is the average delay and $\sigma = \sigma_r\sqrt{2+2\cos(\varphi)}/c$, here φ is the angle between a line from the BS to the center of the cluster and a line from there to the MS, c is the speed of light. The derivation of Eqn.(5) can be found in Appendix A.

Let $f_\alpha(\alpha) = g_\alpha(\alpha)$, $f_\beta(\beta) = g_\beta(\beta)$, $f_\tau(\tau) = g_\tau(\tau)$, then following the derivation in [9], Eqn.(2) can be approximately represented by

$$\begin{aligned} C_{ch}(\kappa, n, d_B, d_M) &\approx \widehat{C}_{ch}(\kappa, n, d_B, d_M) = e^{-2\pi^2\sigma_b^2 \sin^2(\alpha_0) d_B^2} \\ &\cdot e^{j2\pi d_B \cos(\alpha_0)} e^{-2\pi^2\sigma_m^2 \sin^2(\beta_0) d_M^2} e^{j2\pi d_M \cos(\beta_0)} \\ &\cdot e^{-2\pi^2\sigma^2 n^2 \Delta f^2} e^{-j2\pi\overline{\tau} n\Delta f} e^{-2\pi^2\sigma_m^2 \sin^2(\gamma-\beta_0)\kappa^2} \\ &\cdot e^{-j2\pi\kappa\cos(\gamma-\beta_0)} e^{-4\pi^2\sigma_m^2 d_M \sin(\gamma-\beta_0)\sin(\beta_0)\kappa} \end{aligned} \quad (6)$$

Furthermore, the last term of Eqn.(6) could be dropped off if it can be approximated as one. This is the case for small apertures and small angular spreads. Hence, Eqn.(6) can be approximately expressed as

$$\begin{aligned} \widehat{C}_{ch}(\kappa, n, d_B, d_M) &\approx \overline{C}_{ch}(\kappa, n, d_B, d_M) \\ &= \widehat{\rho}_B(d_B)\widehat{\rho}_M(d_M)\widehat{s}_{ch}(n)\widehat{r}_{ch}(\kappa) \end{aligned} \quad (7)$$

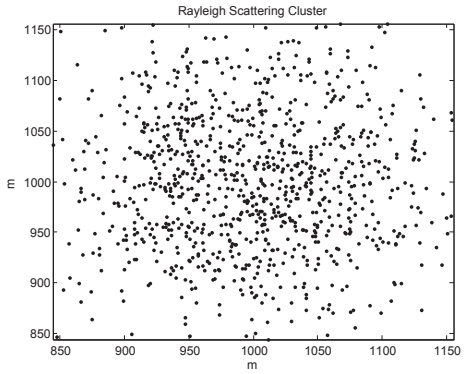

Fig. 3. A DRH Scattering Cluster with Parameters $\sigma_r = 74.33$ and $N = 1000$ Scatterers.

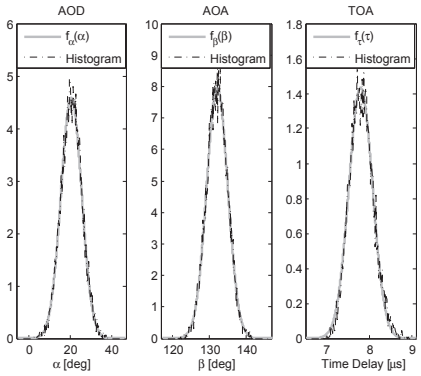

Fig. 4. AOD, AOA, TOA from the DRH Scattering Cluster with Parameters $\sigma_m = 0.05$, $\sigma_b = 0.087$, $\sigma = 0.2781$, $\alpha_0 = 20.56^0$, $\beta_0 = 132.27^0$, $\overline{\tau} = 7.8\ \mu s$ and $N = 10000$ Scatterers.

where

$$\begin{aligned}
\widehat{\rho}_B(d_B) &= e^{-2\pi^2\sigma_b^2\sin^2(\alpha_0)d_B^2}e^{j2\pi d_B\cos(\alpha_0)} \\
\widehat{\rho}_M(d_M) &= e^{-2\pi^2\sigma_m^2\sin^2(\beta_0)d_M^2}e^{j2\pi d_M\cos(\beta_0)} \\
\widehat{s}_{ch}(n) &= e^{-2\pi^2\sigma^2n^2\Delta f^2}e^{-j2\pi\overline{\tau}n\Delta f} \\
\widehat{r}_{ch}(\kappa) &= e^{-2\pi^2\sigma_m^2\sin^2(\gamma-\beta_0)\kappa^2}e^{-j2\pi\kappa\cos(\gamma-\beta_0)}
\end{aligned} \tag{8}$$

Therefore, the 2×2 MIMO-OFDM channel with the channel vector $[h_{11}(t,f)\ h_{12}(t,f)\ h_{21}(t,f)\ h_{22}(t,f)]$ could be approximately modeled by $\widehat{r}_{ch}(\kappa)\widehat{s}_{ch}(n)\mathcal{C}_{MIMO}$, in which

$$\mathcal{C}_{MIMO} = \mathcal{C}_{BS} \otimes \mathcal{C}_{MS} \tag{9}$$

here $\otimes$ denotes the Kronecker product and

$$\begin{aligned}
\mathcal{C}_{BS} &= \begin{bmatrix} 1 & \widehat{\rho}_B(d_B) \\ \widehat{\rho}_B^*(d_B) & 1 \end{bmatrix} \\
\mathcal{C}_{MS} &= \begin{bmatrix} 1 & \widehat{\rho}_M(d_M) \\ \widehat{\rho}_M^*(d_M) & 1 \end{bmatrix}
\end{aligned} \tag{10}$$

IV. AR(3) Approach

In this section, we approach the MIMO channel temporal dynamics by an AR(3) process. This is motivated by the simplicity, efficiency and the correlation matching properties.

A general AR(3) process is given by [17]

$$x_l = \phi_1 x_{l-1} + \phi_2 x_{l-2} + \phi_3 x_{l-3} + w_l \tag{11}$$

where $w \sim \mathcal{N}(0;\sigma_w^2)$, and $\phi_1,\ \phi_2,\ \phi_3$ are coefficients ($\phi_3 \neq 0$). From Eqn.(11), we define the AR(3) operator as

$$\phi(z) = z^3 - \phi_1 z^2 - \phi_2 z - \phi_3 \tag{12}$$

By definition, the autocovariance function for w_l is given by

$$\begin{aligned}
\mathrm{cov}\big(w_l, w_{l-k}^*\big) = \mathrm{cov}\Big(&(x_l - \phi_1 x_{l-1} - \phi_2 x_{l-2} - \phi_3 x_{l-3}), \\
&(x_{l-k} - \phi_1 x_{l-k-1} - \phi_2 x_{l-k-2} - \phi_3 x_{l-k-3})^*\Big)
\end{aligned} \tag{13}$$

where $k = \kappa/\Delta_\kappa$, here $1/\Delta_\kappa$ is the spatial sampling rate per wavelength with $k = \{0, 1, 2, \cdots\}$. It is pointed out that the three roots of Eqn.(12) should lie inside the unit circle for which Eqn.(11) is stable. Obviously, the roots vary within the unit circle depending on Δ_κ.

Define the AR(3) model's coefficients as

$$\begin{cases}
\phi_1 &= \rho_1 e^{-j2\pi\Delta_\kappa\cos(\gamma-\beta_0)} \\
\phi_2 &= \rho_2 e^{-j4\pi\Delta_\kappa\cos(\gamma-\beta_0)} \\
\phi_3 &= \rho_3 e^{-j6\pi\Delta_\kappa\cos(\gamma-\beta_0)}
\end{cases} \tag{14}$$

where $\rho_1,\ \rho_2,\ \rho_3$ are real numbers. The coefficients structure is employed due to the cancellation of the phase terms appeared during the computations in Eqn.(13). Let $E[x_l x_{l-k}^*] = \overline{C}_{ch}(\kappa,0,0,0)$ (Eqn.(7)) and denote $E[w_l w_{l-k}^*] = \delta(k)\sigma_w^2$, then $\rho_1,\ \rho_2,\ \rho_3$ are computed by combining the spectral theory with Eqn.(13) [9]

$$\rho_1 = \frac{(50uv + 55u + 5)\varpi^2 + 360uvp(1-\varpi)}{360uvp + (4uv + 5u + 1)\varpi^2} \tag{15}$$

$$\begin{aligned}
\rho_2 = &- \frac{(4uv + 5u + 1)^2\varpi^4}{360uvp\big(360uvp + (4uv + 5u + 1)\varpi^2\big)} \\
&- \frac{360uvp(4uv + 5u + 1)\varpi^3}{360uvp\big(360uvp + (4uv + 5u + 1)\varpi^2\big)} \\
&- \frac{360uvp\big(50uv + 55u + 5\big)\varpi^2}{360uvp\big(360uvp + (4uv + 5u + 1)\varpi^2\big)}
\end{aligned} \tag{16}$$

$$\rho_3 = \frac{(4uv + 5u + 1)\varpi^2}{360uvp} \tag{17}$$

where $p = 8\pi^2\Delta_\kappa^2\sigma_m^2\sin^2(\gamma - \beta_0)$, $u = \varepsilon p/10$, $v = p/6$ and

$$\varpi = \sigma_w\sqrt{\sigma_m\Delta_\kappa|\sin(\gamma - \beta_0)|\sqrt{2\pi}} \tag{18}$$

here ε is a parameter of adjusting the tails of a 6^{th} order rational function to closer a considered Gaussian PDF. Moreover, an 8^{th} order equation with unknown ϖ is obtained. One could solve it numerically for ϖ. Thus, σ_w is calculated by Eqn.(18).

V. AR(3) Based State Space MIMO Channel Model

In this section, the MIMO channel temporal dynamics, $\widehat{r}_{ch}(\kappa)$, contributed from the DRH scattering cluster has been modeled as an AR(3) process and hence will be realized in state space form. The states are the contribution from the DRH scattering cluster to each channel. The correlated input noises are controlled by $\widehat{s}_{ch}(n)\mathcal{C}_{MIMO}$. There are many ways of doing the state space realization. Here, the Controllable Canonical Form is employed [18].

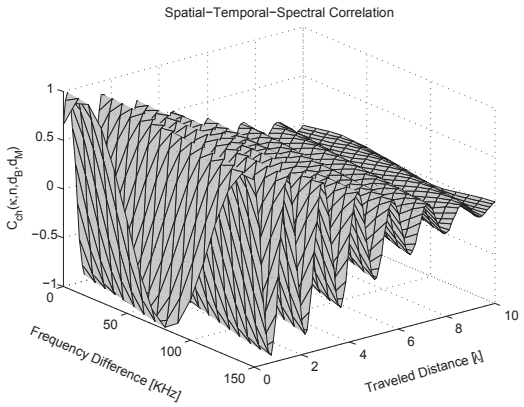

Fig. 5. Real Part of the Spatial-Temporal-Spectral Correlation Function, $\widehat{C}_{ch}(\kappa, n, d_B, d_M)$ (Eqn.(6)), $W_c \approx 99.47$ KHz, $d_B = d_M = \lambda/2$.

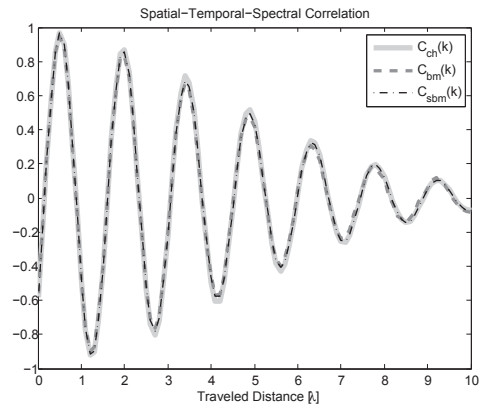

Fig. 6. Real Part of the Channel Spatial-Temporal-Spectral Correlation Function, $E[h_{11}(m, f + l\Delta f)h^*_{22}(m - k, f + q\Delta f)]$, $n\Delta f = 100$ KHz.

Based on the spatial-temporal-spectral correlation function $\overline{C}_{ch}(\kappa, n, d_B, d_M)$ (Eqn.(7)), the MIMO-OFDM channel is represented by state space model

$$\begin{aligned} X_{k+1} &= AX_k + BDW_k \\ H_k &= CX_k \end{aligned} \tag{19}$$

where $X_k \in \mathbb{C}^{12M\times 1}$ is the state vector; $W_k \in \mathbb{C}^{4M\times 1}$ is the $4M$ input iid complex Gaussian noises, in which $w_i \sim \mathcal{CN}(0; 1)$, and W_k, X_k are independent; $H_k \in \mathbb{C}^{4M\times 1}$ is the output vector, the $4M$ channels, which are expressed as $[\mathbf{h}(k, 0)\ \mathbf{h}(k, 1)\ \cdots\ \mathbf{h}(k, M-1)]^T$ for fixed d_B and d_M, here $\mathbf{h}(k, n) = [h_{11}(k, f+n\Delta f)\ h_{12}(k, f+n\Delta f)\ h_{21}(k, f+n\Delta f)\ h_{22}(k, f+n\Delta f)]^T$, M denotes the total number of sub-carrier frequencies; and $A \in \mathbb{C}^{12M\times 12M}$ is the state matrix, $B, D \in \mathbb{C}^{12M\times 4M}$ are the input matrices controlling spatial and spectral correlation, respectively, $C \in \mathbb{R}^{4M\times 12M}$ is the output matrix. The covariance matrix for the innovations can be shown to be

$$BDD^HB^H = \mathcal{C}_{FS} \otimes \left(\mathcal{C}_{MIMO} - \Gamma\mathcal{C}_{MIMO}\Gamma^H\right) \tag{20}$$

A, B, C and D are given by

$$A = \Gamma \otimes I_M,\ B = \Psi \otimes I_M,\ C = \Omega \otimes I_M,\ D = \Lambda \otimes I_4 \tag{21}$$

where I_M is the identity matrix of size M, and $\Gamma \in \mathbb{C}^{12\times 12}$, $\Psi \in \mathbb{C}^{12\times 4}$, $\Omega \in \mathbb{C}^{4\times 12}$ are defined below.

For each state space model block represented the channel vector $\mathbf{h}(k, n)$, Γ, Ψ and Ω are given by [9]

$$\begin{aligned} \Gamma &= \begin{bmatrix} 0 & 1 & 0 \\ 0 & 0 & 1 \\ \phi_3 & \phi_2 & \phi_1 \end{bmatrix} \otimes I_4, \quad \Omega = [0\ 0\ 1] \otimes I_4, \\ \Psi &= \left(\frac{\varpi}{\sqrt{\sqrt{2\pi}\Delta_\kappa \sigma_m |\sin(\gamma - \beta_0)|}} \begin{bmatrix} 0 \\ 0 \\ 1 \end{bmatrix} \otimes I_4 \right) \Phi \end{aligned} \tag{22}$$

where $\Phi \in \mathcal{C}^{4\times 4}$, $\Phi\Phi^H = \mathcal{C}_{MIMO}$ and $\Psi\Psi^H = \mathcal{C}_{MIMO} - \Gamma\mathcal{C}_{MIMO}\Gamma^H$, $(\cdot)^H$ denotes the Hermitian transpose.

For M state space model blocks represented the channel vector $[\mathbf{h}(k, 0)\ \mathbf{h}(k, 1)\ \cdots\ \mathbf{h}(k, M-1)]^T$, Λ is represented by

$$\Lambda\Lambda^H = \mathcal{C}_{FS} \tag{23}$$

where

$$\mathcal{C}_{FS} = \begin{bmatrix} \widehat{s}_{ch}(0) & \widehat{s}_{ch}(1) & \cdots & \widehat{s}_{ch}(M-1) \\ \widehat{s}^*_{ch}(1) & \widehat{s}_{ch}(0) & \cdots & \widehat{s}_{ch}(M-2) \\ \vdots & \vdots & \ddots & \vdots \\ \widehat{s}^*_{ch}(M-1) & \widehat{s}^*_{ch}(M-2) & \cdots & \widehat{s}_{ch}(0) \end{bmatrix} \tag{24}$$

A Cholesky decomposition can be used to numerically obtain the lower triangular matrix Φ and Λ. For the 2×2 system, the elements of Φ are given in [9]. When $M = 2$, for an arbitrary pair of sub-carrier frequencies, D has the following analytical expression (see Appendix B for details)

$$D = \begin{bmatrix} 1 & 0 \\ \widehat{s}^*_{ch}(n) & \sqrt{1 - |\widehat{s}_{ch}(n)|^2} \end{bmatrix} \otimes I_4 \tag{25}$$

VI. Simulations

In this section, to validate the DRH scattering cluster based state space model, a number of numerical simulations are performed, which are given below.

A. Distant Scattering Cluster

In a Cartesian coordinate system, the cluster center C, BS and MS are assumed to be $\mathrm{C}(1000, 1000)$, $\mathrm{BS}(200, 700)$, $\mathrm{MS}(2000, -100)$ with unit meter, then $L_M = 1486.6\ m$, $L_B = 854.4\ m$. Given $\sigma_m = 0.05$, then the DRH scattering cluster is generated from θ and r [1]. Fig.3 displays the cluster with $\sigma_r = 74.33$ and $N = 1000$ scatterers.

B. AOD, AOA, TOA

Given the DRH scattering cluster, we obtain $\alpha_0 = 20.56^0$, $\beta_0 = 132.27^0$ (in the simulations, we simply put both BS and MS antenna arrays along the x-axis), $\overline{\tau} = 7.8\ \mu s$, $\varphi = \beta_0 - \alpha_0 = 111.71^0$, $\sigma_b = 0.087$, $\sigma = 2.781 \times 10^{-7}$. According to the geometrical relations as depicted in Fig.2, the AOD, AOA and TOA are plotted in Fig.4 for $N = 10000$ scatterers. The delay spread of the channels $\tau_{rms} \approx 1.6\ \mu s$, the coherence bandwidth $W_c \geq (2\pi\tau_{rms})^{-1} \approx 99.47$ KHz.

[1]The distribution function of $g_y(y)$ in Eqn.(3) is $F(r) = \int_0^r g_y(y)dy = 1 - \exp(-\frac{r^2}{2\sigma_r^2})$, where r denotes the distance. Let $F(r) = z$, here $z \in [0\ 1)$ is an uniform random variable, then r is generated by $\sigma_r\sqrt{-2\ln(1-z)}$ [19].

C. Channel Correlation

Based on the parameters provided in VI-A, VI-B and $\gamma = 179^0$, $d_B = d_M = \lambda/2$, the spatial-temporal-spectral correlation function, $\widehat{C}_{ch}(\kappa, n, d_B, d_M)$ (Eqn.(6)), is plotted in Fig.5. Given an arbitrary pair of sub-carrier frequencies separated by the coherence bandwidth, the MIMO-OFDM channel simulation scheme is designed as follows.

The analytical correlation function

$$C_{bm}(k) = \sum_{m=1}^{N} |c_m|^2 e^{-j2\pi n \Delta f \tau_m} e^{j2\pi d_B \cos(\alpha_m + \alpha_0)} \cdot e^{j2\pi d_M \cos(\beta_m + \beta_0)} e^{-j2\pi k \Delta_\kappa \cos(\beta_m + \beta_0 - \gamma)} \quad (26)$$

for channels from the DRH scattering cluster is compared to the approached correlation function $\widehat{C}_{ch}(\kappa, n, d_B, d_M)$ and the channel correlation got from the state space model Eqn.(19)

$$C_{sbm}(k) = E[h_{11}(m, f + l\Delta f) h^*_{22}(m - k, f + q\Delta f)] \quad (27)$$

in which $n = q - l$. The results are plotted in Fig.6, on which $C_{ch}(k)$ denotes $\overline{C}_{ch}(\kappa, n, d_B, d_M)$, and $\phi_1 = 2.6335 - 1.2100i$, $\phi_2 = -1.8242 + 2.1249i$, $\phi_3 = 0.2482 - 0.8675i$, $\varpi = 6.381 \times 10^{-5}$.

The spatial-temporal-spectral correlations obtained from the DRH scattering cluster approach and the state space simulations have very similar correlation properties as the theoretical ones.

VII. Conclusions

In this paper, a MIMO-OFDM channel simulator is developed for the environment where the channel spatial-temporal-spectral correlation is due to clustered radio propagation. The scattering clusters are assumed to be 2D DRH clusters. This leads to AOD, AOA and TOA are approximately modeled as the Gaussian angular power density functions and delay power density function. For small angular spread, an AR(3) process has approximately the same channel temporal dynamical properties as the channel contributed from such a cluster. A state space technique is employed to represent the AR(3) process and to handle the spatial correlation properties in the state space form. A lower triangular matrix is used to control the channel spectral correlation properties between the state space forms (blocks). If there are $\mathcal{K}$ uncorrelated state space forms contributing to MIMO-OFDM channels, then the channels can be modeled by simply adding up the $\mathcal{K}$ state space blocks.

Appendix A

Fig.2 shows that the triangles ΔCOB_1 and ΔCOM_1 have the following relationships

$$\frac{r}{\sin(\alpha)} = \frac{OB_1}{\sin(\theta)}, \qquad \tan(\alpha) = \frac{r\sin(\theta)}{L_B - r\cos(\theta)} \quad (28)$$
$$\frac{r}{\sin(\beta)} = \frac{OM_1}{\sin(\theta + \varphi)}, \ \tan(\beta) = \frac{r\sin(\pi - (\theta + \varphi))}{L_B + r\cos(\pi - (\theta + \varphi))}$$

For small angles α, β, we get that $\sin(\alpha) \approx \alpha$, $\tan(\alpha) \approx \alpha$, $\sin(\beta) \approx \beta$ and $\tan(\beta) \approx \beta$. Associated with $\tau = (OM_1 + OB_1)/c$ and Eqn.(28), we have $r \approx \frac{c\tau - L}{\sqrt{2+2\cos(\varphi)}\cos(\theta+\omega)}$ and $\frac{dr}{d\tau} \approx \frac{c}{\sqrt{2+2\cos(\varphi)}\cos(\theta+\omega)}$, where $\omega = \arccos\big((1 + \cos(\varphi))/\sqrt{2 + 2\cos(\varphi)}\big)$, $L = L_M + L_B$. Substituting, in Eqn.(3), the random variable r by the time delay τ gives

$$g_{\theta,\tau}(\theta, \tau) \approx \frac{1}{2\pi} \frac{c(c\tau - L) e^{-\frac{(c\tau - L)^2}{2(2+2\cos(\varphi))\cos^2(\theta+\omega)\sigma_r^2}}}{(2 + 2\cos(\varphi))\cos^2(\theta + \omega)} \quad (29)$$

then Eqn.(5) is obtained by taking the integration to Eqn.(29) w.r.t. θ [9]. The angle φ can be computed from the triangle $\Delta B_1 C M_1$ in Fig.2. That is, $\cos(\varphi) = \frac{L_B^2 + L_M^2 - B_1 M_1^2}{2 L_B L_M}$.

Appendix B

Let $D = \begin{bmatrix} d_{11} & 0 \\ d_{21} & d_{22} \end{bmatrix} \otimes I_4$, then

$$\Lambda\Lambda^H = \begin{bmatrix} |d_{11}|^2 & d_{11}d^*_{21} \\ d^*_{11}d_{21} & |d_{21}|^2 + |d_{22}|^2 \end{bmatrix} = \begin{bmatrix} 1 & \widehat{s}_{ch}(n) \\ \widehat{s}^*_{ch}(n) & 1 \end{bmatrix} \quad (30)$$

Solving Eqn.(30) gives Eqn.(25).

References

[1] Richard B. Ertel and Jeffrey H. Reed, "Angle and Time of Arrival Statistics for Circular and Elliptical Scattering Models," *IEEE J. on Selected Areas in Communications,* Vol. 17, No. 11, 1999.

[2] Juha Laurila, Andreas F. Molisch and Ernst Bonek, "Influence of the Scatterer Distribution on Power Delay Profiles and Azimuthal Power Spectra of Mobile Radio Channels," *IEEE 5th International Symposium on Spread Spectrum Techniques and Applications,* 1998.

[3] Paul Petrus, Jeffrey H. Reed and Theodore S. Rappaport, "Geometrically Based Statistical Channel Model for Macrocellular Mobile Environments," *GLOBECOM '96. 'Communications: The Key to Global Prosperity,* 1996.

[4] Ramakrishna Janaswamy, *Radiowave Propagation and Smart Antennas for Wireless Communications,* Kluwer Academic Publishers, 2001.

[5] G. Stüber, J. Barry, S. McLaughlin, Y. Li, M. Ingram and T. Pratt, "Broadband MIMO-OFDM Wireless Communications," *Proceedings of the IEEE,* Vol. 92, No. 2, 2004.

[6] Xin Li, *State Space Estimation of Wireless Fading Channels,* Master's Thesis, University of Ottawa, Canada, 2002.

[7] C. D. Charalambous, R. J. C. Bultitude, X. Li and J. Zhan, "Modeling Wireless Fading Channels via Stochastic Differential Equations: Identification and Estimation Based on Noisy Measurements," *IEEE Transactions on Wireless Communications,* Vol. 7, No. 2, 2008.

[8] K. J. Kim and T. Reid, "Multiple Hypothesis Cannnel Estimation for the MIMO-OFDM System," *IEEE Globecom,* 2004.

[9] Xin Li and Torbjörn Ekman, "Gaussian Angular Distributed MIMO Channel Model" *IEEE VTC Fall,* 2011.

[10] Xin Li and Torbjörn Ekman, "Cauchy Power Azimuth Spectrum for Clustered Radio Propagation MIMO Channel Model", *IEEE VTC Fall,* 2010.

[11] E. Kunnari and J. Linatti, "Stochastic Modeling of Rice Fading Channels with Temporal, Spatial and Spectral Correlation", *IET Communications,* Vol. 1, No. 2, 2007.

[12] A. F. Molisch, *Wireless Communications,* John Wiley & Sons, Inc., 2005.

[13] W. C. Y. Lee, *Mobile Communications Engineering,* McGraw – Hill Book Company, 1982.

[14] K. Kalliola, K. Sulonen, H. Laitinen, O. Kivekäs, J. Krogerus and P. Vainikainen, "Angular Power Distribution and Mean Effective Gain of Mobile Antenna in Different Propagation Environments", *IEEE Transactions on Vehicular Technology,* Vol. 51, No. 5, 2002.

[15] C. Chong, C. Tan, D. I. Laurenson, S. McLaughlin, M. A. Beach and A. R. Nix, "A New Statistical Wideband Spatio-Temporal Channel Model for 5-GHz Band WLAN Systems", *IEEE Journal on Selected Areas in Communications,* Vol. 21, No. 2, 2003.

[16] Torbjörn Ekman, *Prediction of Mobile Radio Channels,* PhD Thesis, Uppsala University, Sweden, 2002.

[17] Robert H. Shumway and David S. Stoffer, *Time Series Analysis and Its Applications,* 2^{nd}, Springer, 2006.

[18] Katsuhiko Ogata, *Modern Control Engineering,* 3^{rd}, Prentice-Hall Inc., 1996.

[19] Luc Devroye, *Non-uniform Random Variate Generation,* Springer-Verlag New York Inc., 1986.